Numerical simulation of the effect of flow field in swirl nozzle spinning on yarn performance

DOI: 10.35530/IT.070.06.1422

JIANG YAN HUA QIU

ABSTRACT – REZUMAT

Numerical simulation of the effect of flow field in swirl nozzle spinning on yarn performance

Swirl nozzle spinning is an effective method to reduce ring-spun yarn hairiness due to device structure and vortex characteristics. This study establishes a computational domain of a swirl nozzle comprising an air inlet channel and a yarn channel to investigate the characteristics of the vortex in the swirl nozzle and the effects of inlet pressure on the wrapped force of the yarn. Simulation results show that the airflow rotates clockwise toward the two yarn entrance directions; moreover, the pressure at the central area of the yarn channel is lower than that of the surrounding area, which is good for the yarn's steady movement and free fibers wrapping on the yarn surface into the yarn body. When the inlet pressure is high, the pressure spreading to each section of the yarn channel is also high. When the difference between the pressure near the inner wall and the yarn axis is high, the yarn surface has added high pressure, and the velocity and its fluctuation are also high. Experiment result reveals that 0.2 MPa is sufficient in significantly reducing yarn hairiness and that operating the nozzle under a low air pressure is economical. Thus, the numerical simulation can provide the theoretical as well as quantitative reference for the vortex tube design in the coming future.

Keywords: *swirl nozzle, vortex, hairiness, free fiber, inlet pressure*

Simularea numerică a influenţei câmpului de curgere în filarea cu duze în spirală asupra performanței firului

Filarea cu duze în spirală este o metodă eficientă pentru a reduce pilozitatea firelor filate cu inele datorită structurii dispozitivului și a caracteristicilor sistemului Vortex. Acest studiu stabilește un domeniu de calcul al parametrilor de proiectare a duzelor în spirală, care sunt formate dintr-un canal de intrare a aerului și un canal de fire, pentru a investiga caracteristicile sistemului Vortex în duza în spirală și influenţa presiunii de intrare asupra forței de înfășurare a firului. Rezultatele de simulare arată că fluxul de aer se rotește în sens orar spre cele două direcții de intrare ale firelor; în plus, presiunea în zona centrală a canalului de conducere a firelor este mai mică decât cea a zonei înconjurătoare, ceea ce este corespunzător pentru mișcarea uniformă a firelor și înfășurarea fibrelor libere pe suprafața firelor în corpul firelor. Când presiunea de intrare este ridicată, presiunea distribuită pe fiecare secțiune a canalului de conducere a firelor este, de asemenea, ridicată. Când diferența dintre presiunea din apropierea peretelui interior și presiunea din axa firelor este mare, suprafața firelor prezintă o presiune ridicată, iar viteza și fluctuația sa sunt, de asemenea, ridicate. Rezultatul experimentului arată că o valoare de 0,2 MPa este suficientă pentru a reduce semnificativ pilozitatea firelor, iar funcționarea duzei la o presiune scăzută a aerului este economică. Astfel, simularea numerică poate oferi o referință teoretică, precum și cantitativă pentru proiectarea tubului vortex în viitorul apropiat.

Cuvinte-cheie: *duză în spirală, vortex, pilozitate, fibră liberă, presiune de intrare*

INTRODUCTION

Yarn hairiness is a key factor affecting yarn and fabric processes and properties. Some new technologies have been developed to reduce the hairiness of ring spun yarns, such as compact spinning [1–2], jet ring spinning [3] and the use of a contact surface or air nozzle [4]. Initially introduced in 2012, swirl nozzle spinning is a novel method to reduce ring yarn hairiness [5]. Vortex nozzle ring spinning is composed of a yarn channel and an air jet nozzle, and it is attached to a traditional ring spin frame (figure 1). When compressed air from the air jet nozzle to the yarn duct is applied, the swirling airflow tucks the surface fibers of the ring-spun yarn into its body to decrease yarn hairiness. Compared with the other methods above, swirl nozzle spinning is simple to install, easier to operate, and cost lower. This method

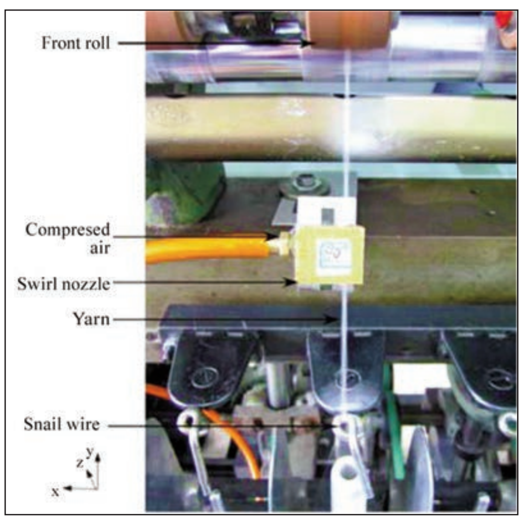

Fig. 1. Swirl nozzle and Installation

has a remarkable capacity in reducing hairiness [6]. Some studies on reducing ring-spun yarn hairiness have been conducted through experimental methods, but the mechanism remains unclear. Therefore, the present work focused on investigating the effect of airflow in the nozzle and different air inlet pressure on the fiber of the yarn surface using numerical and experimental methods. Numerical simulation can provide the theoretical basis for the experiment result, which plays an important role in optimizing the structure of the nozzle and test parameters.

NUMERICAL SIMULATION

Simulation model

Figure 2, *a* presents the 3D geometric model of a swirl nozzle, including the airflow inlet and yarn guide channels. In the figure, compressed air flows into the yarn path from the air inlet. When the airflow arrives at the junction of the airway and yarn path, it reaches a relatively high pressure. Subsequently, the air vortex possessing axial and circumferential velocities is simultaneously generated in the yarn path to make the yarn hairiness stick take before flowing out from the two outlets. The corresponding Outlets 1 and 2 are simultaneously the exits of the airflow and the import and export of the yarn. Figure 2, *b* shows the structural parameters of the swirl nozzle. Airway tangents clockwise to the yarn path, which divides the yarn into two unequal parts. Airway diameter is smaller than that of the yarn path.

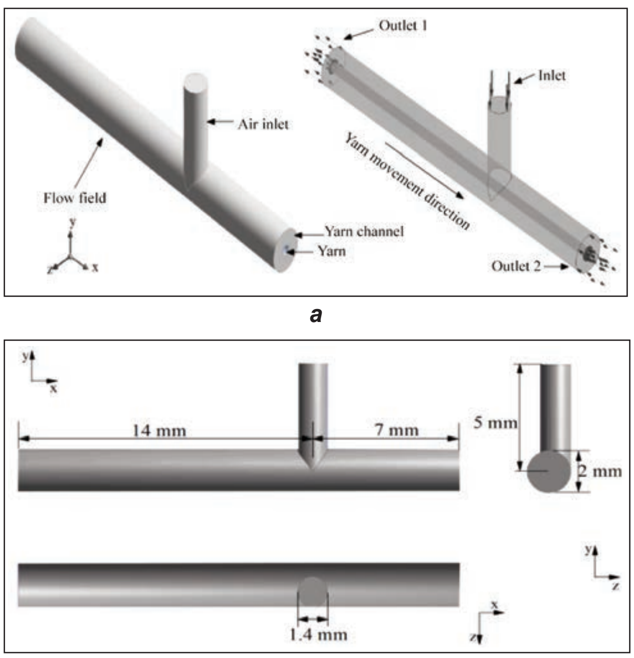

Fig. 2. Fluid domain parameter of the swirl nozzle: *a* – fluid domain of the swirl nozzle; *b* – three view drawing of fluid domain of the swirl nozzle

Method of numerical simulation

Simulation method combined with theoretical analysis and experimental method is widely used to solve application problems in textile, thereby improving the efficiency of problem solving [7–9]. In this study, CFX (CFD software) is used to simulate the airflow in the swirl nozzle. The computational domain is meshed using an unstructured tetrahedral grid. Inflation layer is used inside the yarn channel wall to provide a more accurate prediction of flow characteristics [10]. In addition, the airflow is considered as viscous and incompressible. Turbulence model is adopted for the turbulence.

Boundary conditions

The simulation model is a computational domain with a fluid inlet and two outlets. Various inlet pressures are set. The pressure, temperature, and velocity of the inlet are set as follows:

$$P_{in} = (p + 0.1013) \times 0.528 \quad (1)$$

$$T_{in} = 0.833T \quad (2)$$

$$v_{in} = \sqrt{\gamma R T_{in}} \quad (3)$$

Where p is the pressure in the store jar (p = 0.05, 0.10, 0.15, 0.20, 0.25 MPa), T – atmospheric temperature (T = 293 K), γ is specific heat capacity (for ideal gas, γ = 1.4), R – universal gas constant (R = 287.1 J/Kg·K).

The outlet pressure is equal to the atmospheric pressure (0.1013 MPa). All walls are regarded as non-slip, and an adiabatic boundary condition is imposed in the calculation area; thus, the flow velocity is zero and no heat transfer occurs at the wall. The yarn material is considered as structural steel, and airflow cannot pass into the yarn interior; thus, yarn deformation is ignored.

RESULT AND DISCUSSION

Characteristics of the swirl nozzle vortex

Figure 3 shows the flow trajectories of the compressed air in the swirl nozzle. As illustrated, a blast of compressed air flows from the air inlet into the yarn channel. The airflow along the circular yarn channel rotates and generates a strong vortex composed of circumferential and axial velocities and exits from the two outlets. Moreover, the airflow immediately enters the yarn channel from the air inlet, the pressure of the

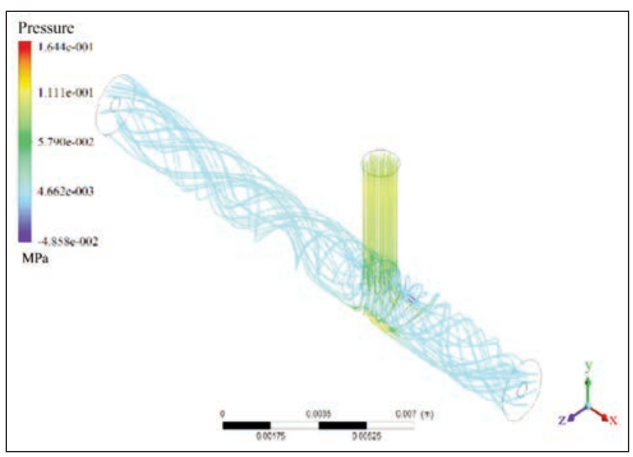

Fig. 3. Flow trajectories in the swirl nozzle

yarn channel wall peaks and then gradually reduces gradually to flow into the outlets. The pressure at the central area of the yarn channel is lower than that of the surrounding area, which is good for the yarn's steady movement.

The rotating channels on both sides are an asymmetrical structure; thus, the distances of the air inlet to two outlets differ. The longer distance is of the untwisted area; the airflow rotates clockwise toward the yarn entrance direction, which is in the opposite direction of the yarn twist direction. The shorter distance is of the re-twisted area; the airflow rotates clockwise to the yarn exit direction, which is in the same direction of yarn twist direction.

As plotted in figure 4, *a*, yarn twist zone and twist zone length differ; to analyze the vortex characteristics, 15 cross-sections of the rotating channel are extracted. As shown, section O-O is selected to describe the airflow characteristics, which immediately enters the rotating channel from the air inlet. Section H-H and F′-F′ are chosen because it is located near the outlet of the rotating channel, where yarn enters and exits. The rest of sections are placed to observe the development of the vortex.

Figure 4, *b* presents the distribution of velocity vector in diferent cross-sections while the inlet pressure is set to 0.5 MPa. The two symmetrical sections have the same velocity vector distributions, where an obvious vortex is evident. As shown, longer arrow means faster airflow velocity; high velocity airflow distributes around the surface of the yarn, which is advantageous for wrapping long fibers of yarn surface. In addition, the circumferential velocity decreases along the two sides of the rotating channel.

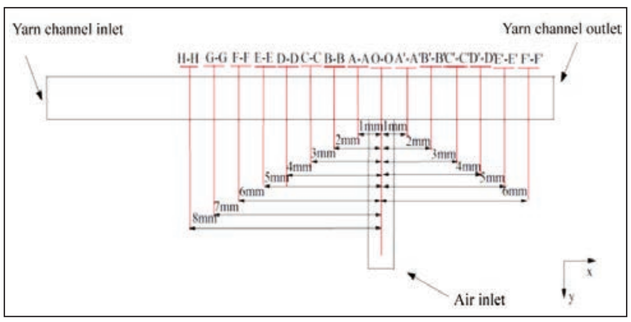

a

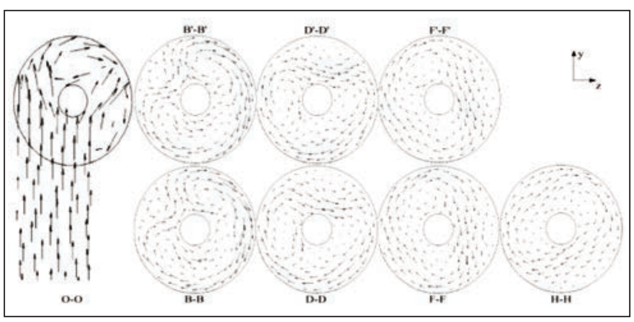

b

Fig. 4. Circumferential velocity vector in the yarn channel: *a* – cross sections of the yarn channel in different positions; *b* – circumferential velocity vector in the yarn channel in various cross-section

Effects of the vortex on the fiber on the yarn surface

As shown in figure 5, the forces generated by the airflow are the wrapped forces *F* and *F*′, which are the resultant forces of *F*1 (along the *x*-axis), *F*2 (along the *y*-axis), and *F*3 (along the *z*-axis), and *F*1′ (along the *x*-axis), *F*2′ (along the *y*-axis), and *F*3′ (along the *z*-axis), respectively. In addition, the relative revolving action F_r and F_r1' is also applied on the free end of fiber due to the self-twisting of the yarn. Thus, the total wrapped forces F_T and F_T' acting on the fibers on the yarn surface can be obtained as follows:

In the untwisted area, airflow acts on the consequent hairiness mainly as follows:

$$F_T = F + F_r' \quad (4)$$

$$F_T = F + F_r' \; \vec{F} = \vec{F1} + \vec{F2} + \vec{F3} \quad (5)$$

In the re-twisted area, airflow acts on the consequent hairiness mainly as follows:

$$F_T' = F' + F_r1' \quad (6)$$

$$\vec{F'} = \vec{F1'} + \vec{F2'} + \vec{F3'} \quad (7)$$

According to the formula of flow around the cylinder, the forces generated by the airflow are related to pressure and airflow velocity [11].

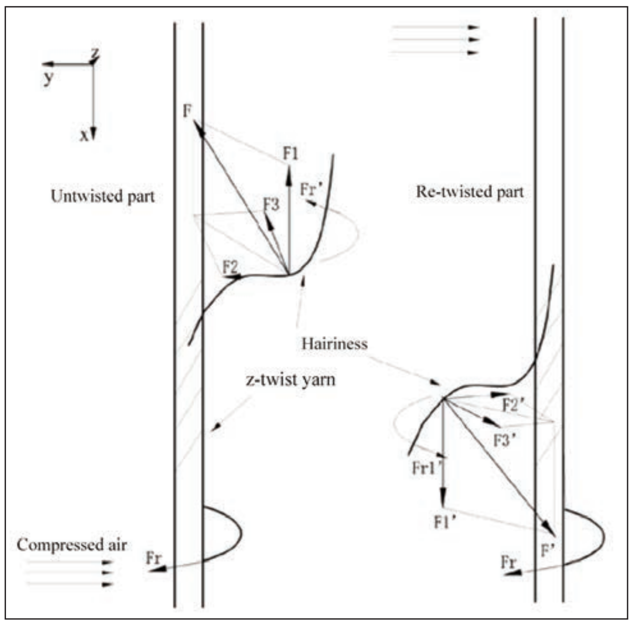

Fig. 5. Force schematic diagram of the yarn under the airflow condition

Effects of inlet pressure on the wrapped force of the yarn

Considering that yarn requires the proper wrapping force to attach yarn hairiness, the comparisons of the vortex pressure in the different cross-sections under diferent inlet pressures with 0.05, 0.10, 0.15, 0.20, and 0.25 MPa are presented in figure 6, *a*. As shown, the negative pressure zone produced by the airflow acting on the yarn at the yarn channel entrance spreads progressively small with the increase in inlet pressure; this phenomenon occurs because when the inlet pressure is higher, the pressure spreading to each section of the yarn channel is higher; the subsequent greater pressure difference existing near the inner wall and yarn axis makes for an easier hold of the yarn, thereby resulting in its steady movement and effective functioning as wrapping fibers. Hair is subjected to a higher total air pressure due to a reducing pressure gradient from the inner wall of the yarn channel to the axis.

Figure 6, *b* shows the yarn surface in the simulated nozzle under different air pressures. Clearly, yarn surface has added high pressure area with the increase in inlet pressure and high and low pressure alternating distribution, thereby easily wrapping the free fibers into the yarn body. However, a significant high pressure would break the yarn structure and blow away some free fibers, which may cause fiber loss. Thus, the air pressure should be properly selected in the actual processing.

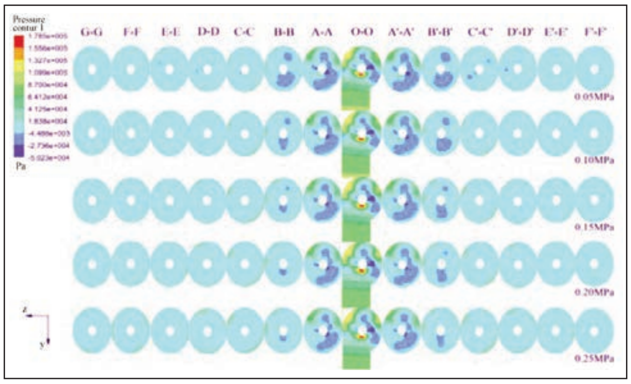

a

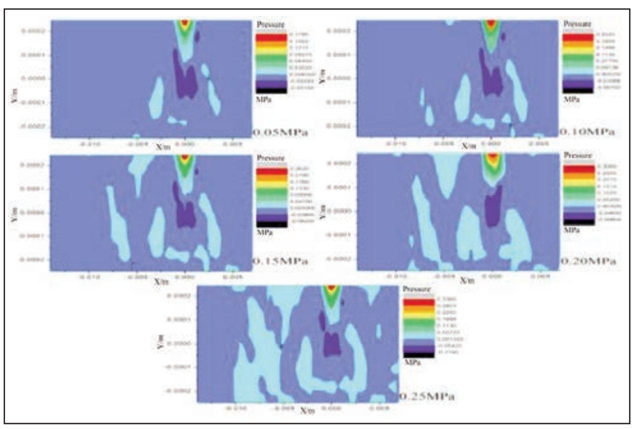

b

Fig. 6. Pressure distribution of swirl nozzle and yarn surface: *a* – pressure distribution in various yarn channel sections under different pressure conditions; *b* – pressure distribution of yarn surface under different pressure conditions

Wrapped force acting on the yarn surface is known to depend on the surface pressure and velocities *u*, *v*, and *w*. Four lines on the yarn surface are selected as the research objects to study the effect of inlet pressure on yarn; the lines are marked Line A, Line B, Line C and Line D, as shown in figure 7.

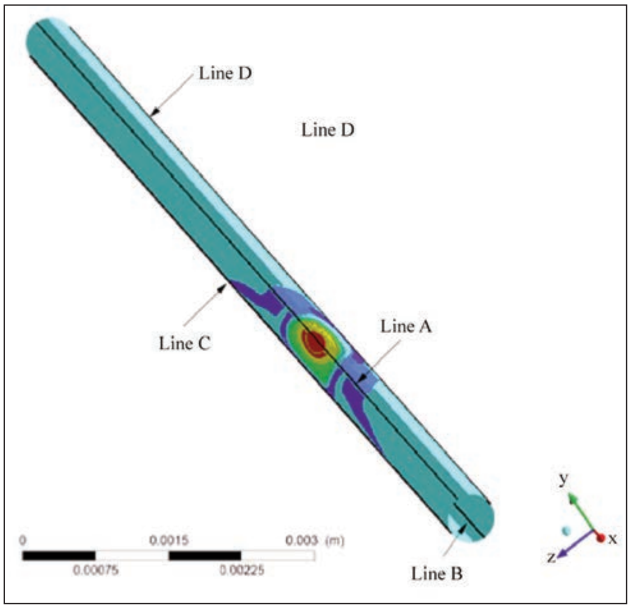

Fig. 7. Position of the four lines selected from the yarn surface

Figure 8 shows the pressure of air acting on the yarn surface under different inlet pressures. The total pressure trend acting on the yarn under different inlet pressure levels are similar. For Line A, the air comes from the air entrance; whereas the pressure suddenly increases near the wall of the yarn channel. This sudden increase in pressure is due to the generation of shock waves, which changes the direction of the airflow movement and creates a swirling effect toward two directions. Then, the pressure decreases due to the presence of two air exits, where air diffuses very quickly and then stabilizes gradually. Under different inlet pressures, the impact of airflow acting on the yarn is greater in the junction of the yarn channel and airway with the increase of inlet pressure. Pressure difference becomes gradually smaller with air flowing out the yarn channel. The pressure generated by Line B increases and decreases; a higher inlet pressure means a greater pressure fluctuation. To some extent, this trend of pressure is advantageous to wrap yarn surface fibers and push down the fiber of the yarn surface from a high-pressure area to a low-pressure area. Lines C and D located on the two sides of the yarn surface have a similar change trend, which generates a high negative pressure, subsequently undergoes pressure recovery, and eventually levels off. Inlet air pressure affects the negative pressure and air pressure fluctuation. To sum up, the yarn surface requires moderate pressure; if too low, the force is insufficient to wrap the yarn; if too high, the free fibers are easily blown away, thereby causing fiber loss and yarn tenacity.

The total air velocity acting on the yarn is resolved into velocity *u* (along the *x*-axis), velocity *v* (along the *y*-axis), and velocity *w* (along the *z*-axis). Velocity *u* holds the yarn and makes it move steadily. Velocities *v* and *w* play the function of attaching and wrapping free fibers on the yarn surface [12]. Figure 9 shows the axial component of the air velocity on the yarn surface under various inlet pressures inside the nozzle. Four lines have similar trends on velocity *u*; whereas axial air velocity suddenly increases near the yarn channel. Then, axial velocity decreases with air flowing out the two exits. Thus, the delivery effect of airflow on the yarn is becoming smaller. For different inlet pressures, no difference exists in a short distance while entering the yarn channel; then, pressure increases with air flowing to the exits. A higher pressure and greater speed at some point means closer to export and more evident difference.

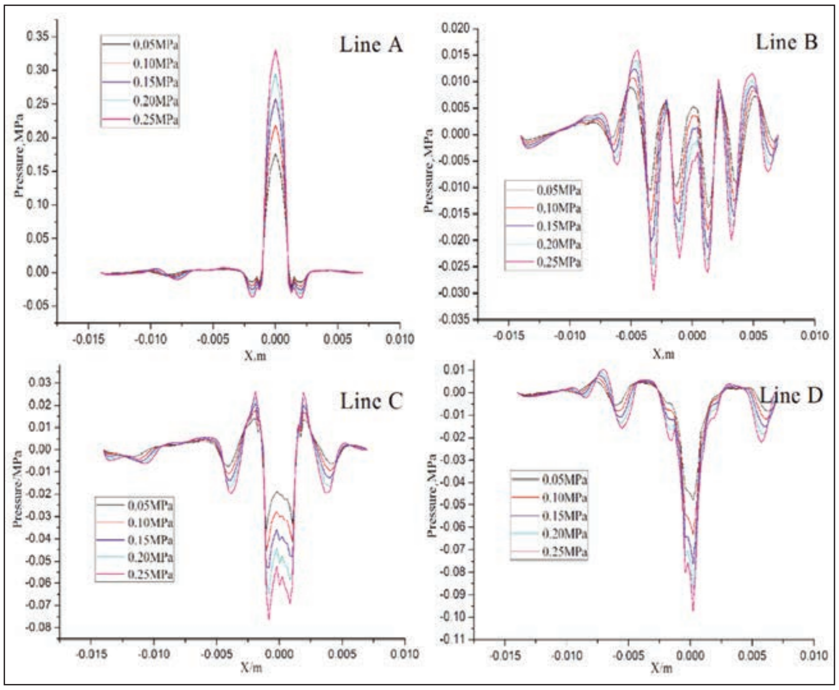

Fig. 8. Pressure distribution of the four lines located on the yarn surface under different pressure conditions

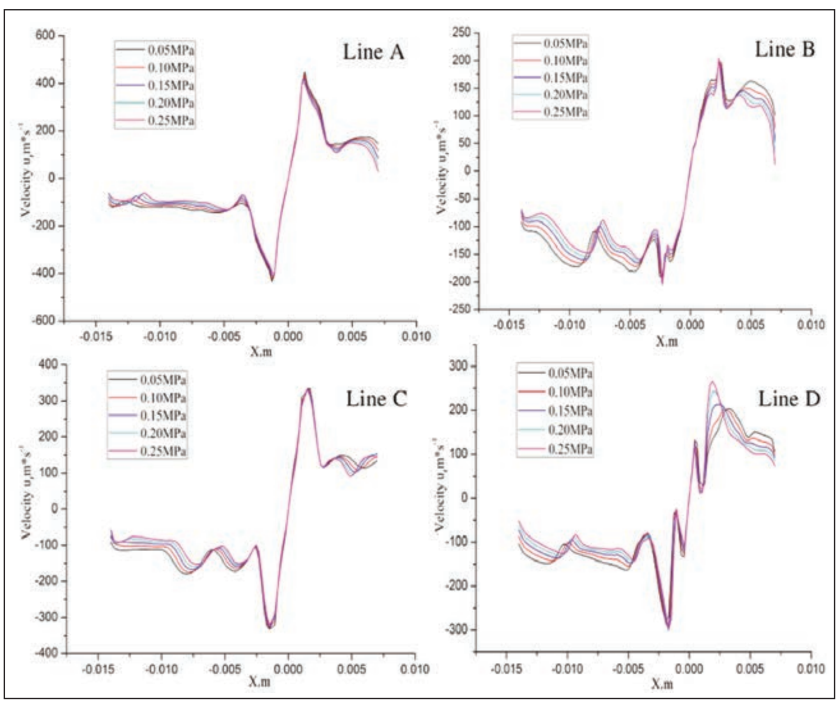

Fig. 9. Velocity *u* distribution of the four lines located on the yarn surface under different pressure conditions

Velocity *v* (along the *y*-axis) and velocity *w* (along the *z*-axis) play the function of opening the yarn structure and wrapping free fiber into the yarn body. Figure 10 shows the y-axis component of the air velocity on the yarn surface under various inlet pressures inside the nozzle. For Lines A and B, Y axial velocities are irregular wavy lines. The significant fluctuation in Line B indicates that the air at the bottom of the yarn velocity changes more along the *x*-axis. The force acting on each position is uneven, which is good for attaching the surface free fibers. Compared with Lines A and B, Lines C and D have smaller changes, except that the velocity in $x = 0$ is high. This phenomenon occurs because the air flow inlet direction moves toward the negative direction of the *y*-axis. Different inlet air pressures create different velocities on the y-direction. A higher inlet pressure means faster speed; however, the overall difference is not evident.

The graph for Line A in figure 11 indicates a great speed fluctuation when the inlet pressure is high. A large difference in velocity is known to have an increased advantage to the wrapped yarn. A higher speed can also create a more sufficient opening for the yarn structure and increase the likelihood of the fiber to be posted on the yarn surface. Under different inlet pressure levels, the fluctuation of velocity *w* of Lines B, C, and D is smaller than that of Line A.

EXPERIMENTAL METHOD

An experimental bench was designed to verify the numerical simulation results. Yarn performance tests based on conventional ring spinning and swirl nozzle spinning were designed to validate the effect of airflow on the yarn hairiness. Alternately, a hairiness tester was used to measure the yarn hairiness index under different inlet pressures, thereby verifying the reasonableness of the theoretical analysis presented in the above section.

The corresponding experimental parameters are listed in table 1. Four types of yarns were produced. Two of these yarns were spun using the conventional ring-spinning system (Samples 1 and 3), whereas the other two yarn were spun using a ring-spinning machine with a vortex nozzle

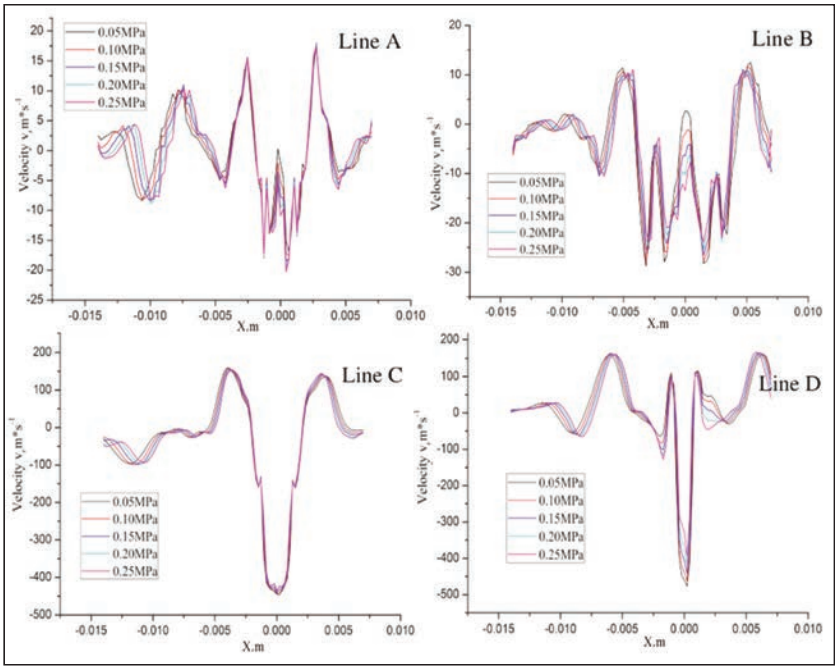

Fig. 10. Velocity *v* distribution of the four lines located on the yarn surface under different pressure conditions

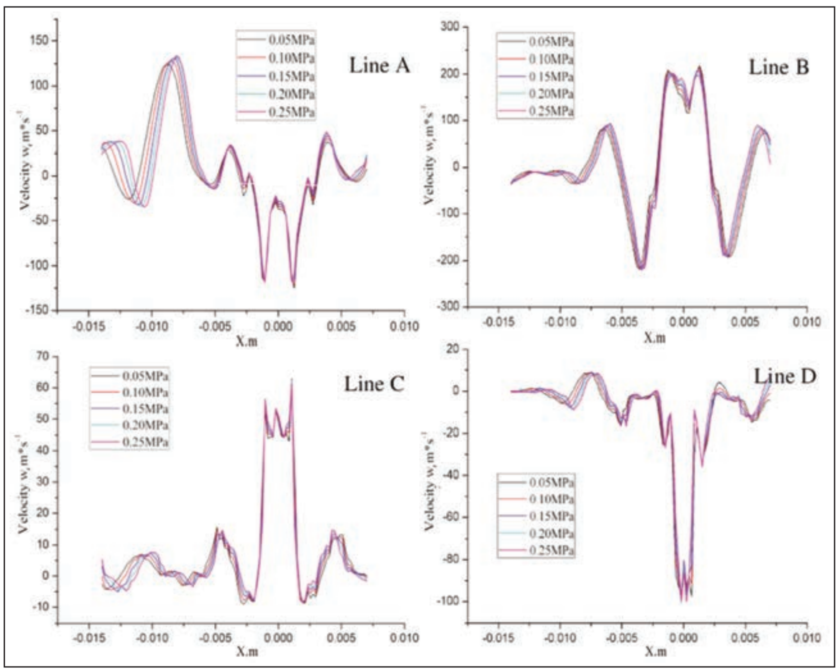

Fig. 11. Velocity *w* distribution of the four lines located on the yarn surface under different pressure conditions

installed between the front roller and the yarn guide of a CZJF-5 multi-function spinning frame (Samples 2 and 4). Samples 1 and 2, as well as Samples 3 and 4, possessed the same roving and spinning process parameters and were spun into the same specifications.

Yarn hairiness was measured on a YG172A hairiness meter, with reference to the industry standard FZ/T 01086-2000 (the determination method of textile yarn hairiness is the projection-counting method).

The hairiness index (number of hairs on the yarn with a length equal to or exceeding 3 mm per meter) was used as the means to compare the hairiness level among the different yarns. The hairiness index of yarns spun with and without the vortex nozzle apparatus were compared, as shown in figure 2. Clearly, the hairiness index of vortex-nozzle-spun yarns is less than those of conventionally spun yarns under different air pressure values. The hairiness index under an air pressure of 0.2 MPa is less than those under other air pressure values. With increasing air pressure, the vortex nozzle has a more obvious effect on reducing hairiness at less than 0.2 MPa. Beyond 0.2 MPa, the yarn hairiness number increases. Thus, an air pressure of 0.2 MPa is clearly sufficient in reducing the yarn hairiness, and operating the nozzle at a low air pressure is also economical.

Simulation and experiment results show that yarn hairiness index decreases with the increase of inlet pressure from 0.05 MPa to 0.2 MPa. The high pressure creates

Table 1

SPINNING EXPERIMENT PARAMETERS					
Sample number	**Yarn type**	**Material**	**Linear density (Tex)**	**Twist factor**	**Spindle speed (rpm)**
Sample 1	Conventional yarn	20% hemp, 80% cotton	30	450	9000
Sample 2	Vortex nozzle yarn	20% hemp, 80% cotton	30	450	9000
Sample 3	Conventional yarn	20% hemp, 80% cotton	30	500	9000
Sample 4	Vortex nozzle yarn	20% hemp, 80% cotton	30	500	9000

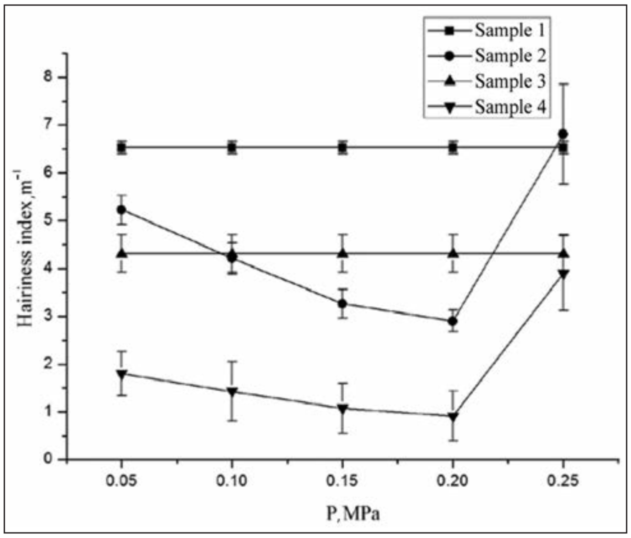

Fig. 12. Comparison of the hairiness index of yarns under different air pressures

a more efficient untwist and re-twist actions; in addition, a stronger wrapped force acts on the yarn surface. However, if the inlet pressure is significantly high, the yarn structure may be blown away and loosened, which will cause a significant loss of fibers and will influence yarn quality.
In order to study the effect of swirl nozzle on other yarn performances at the same time of reducing yarn hairiness under 0.2 MPa air pressure, such as strength, unevenness and the number of short hairiness, breaking strength, unevenness and short hairiness number of four samples were tested, the results showed in table 2. Yarn tenacity was determined on an YG063 automatic single yarn strength tester. Yarn unevenness was measured on YG135G automatic unevenness measurement device.

Table 2

STUDY THE EFFECT OF SWIRL NOZZLE ON OTHER YARN PERFORMANCES

Sample number	Number of short hairiness (1-2 mm)	Breaking strength	Unevenness
Sample 1	61.96	226.2	11.51
Sample 2	72.3	201.2	12.95
Sample 3	69.9	242	11.45
Sample 4	82.4	215.6	13.5

As shown in table 2, swirl nozzle increase the number of short hairiness as well as yarn unevenness slightly, and decrease the yarn strength. More short hairiness will not affect the quality of yarn and subsequent processing, which makes the yarn and fabric feel fuller. Despite swirl nozzle deteriorate yarn strength and evenness, but the difference is not obvious, and the yarn still meets the requirements of Grade A quality according to standard FZ/T 32004-2009.

CONCLUSION

A process of hairiness reduction is explained with the assistance of CFD. The swirling effect of air caused by the nozzle design mainly explains hairiness reduction. Air inlet pressure is an influencing factor in reducing yarn hairiness. The conclusions of this study can be drawn as follows:
(1) The numerical simulation shows the vortex characteristics in the swirl nozzle. The airflow rotates clockwise toward the two yarn entrance directions; moreover, the pressure at the central area of the yarn channel is lower than that of the surrounding area, which is good for the yarn's steady movement and wrapping of free fibers on the yarn surface into the yarn body. The upward movement of the airflow stick takes consequent hairiness and opens the yarn structure; whereas the downward movement of the airflow stick takes reverse hairiness and wraps the fiber into the yarn body.
(2) The forces generated by the airflow acting on the yarn are the wrapped force and the relative revolving action due to the self-twisting of the yarn, which works together to reduce yarn hairiness on the surface.
(3) Numerical simulation reveals the pressure of different yarn channel cross-sections and yarn surface with the increase in the inlet pressure. When the inlet pressure is higher, the pressure spreading to each section of the yarn channel is also higher, and the greater the pressure difference near the inner wall and yarn axis, thereby creating an easier hold for the yarn and then cause its steady movement and effective functioning as wrapping fibers. Furthermore, the velocity along the *x*-, *y*-, and *z*-axes of the four lines on the yarn surface are revealed. No significant difference is observed in the trends of the four lines; however, velocity and velocity fluctuation are higher under a higher inlet pressure.
(4) Experiment result indicates that the hairiness index of vortex-nozzle-spun yarns is less than those of conventionally spun yarns under different air pressure values. The hairiness index under 0.2-MPa air pressure is less than those under other air pressure values. With increasing air pressure, the vortex nozzle has a more obvious effect on reducing hairiness at less than 0.2 MPa. Beyond 0.2 MPa, the yarn hairiness number increases. Swirl nozzle increase the number of short hairiness slightly, which makes yarn feel fuller. It is also deteriorate yarn strength and evenness, but the difference is not obvious.
(5) Numerical simulation and experiment results indicate that a high inlet pressure creates a more significant effect of reducing hairiness. However, if the inlet pressure is remarkably high, the yarn structure may be easily blown away and loosened, which will cause significant loss of fibers and will influence yarn quality. Thus, an air pressure of 0.2 MPa is clearly sufficient

in significantly reducing yarn hairiness, and operating the nozzle at a low air pressure is also economical. This work envisions extending its future investigations on the other important factors and interactive efects of these factors to conduct other comprehensive research.

ACKNOWLEDGEMENTS

The authors are grateful for the financial supported by Prospective Industry-university-research Project of Jiangsu Province (BY2016022-14) and the Fundamental Research Funds for the Central Universities (No. JUSRP51301A).

REFERENCES

[1] Stalder, H., Rusch, A., *Compact spinning wins market acceptance*, In: International Textile Bulletin-English Edition, 2002, 48, 1, 42–43

[2] Cheng, K.P.S., Yu, C., *Compact spinning wins market acceptance*, In: Textile Research Journal, 2003, 73, 4, 345–349

[3] Cheng, K.P.S., Li, C.H.L., *JetRing spinning and its influence on yarn hairiness*, In: Textile Research Journal, 2002, 72, 12, 1079–1087

[4] Xia, Z., Xu, W., Zhang, M., *Reducing ring spun yarn hairiness via spinning with a contact surface*, In: Fibers and Polymers, 2012, 13, 5, 670–674

[5] Qiu, H., Zhang, Y., Xu, Z.L., *A novel method to reduce hairiness level of ring spun yarn*, In: Fibers and Polymers, 2012, 13, 1, 104–109

[6] Qiu, H., Luan, Q., Jiang, H., *Effect of airway angle of a swirl nozzle on performance of ring-spun yarn*, In: Industria Textila, 2016, 67, 1, 10–16

[7] Rengasamy, R.S., Patanaik, A., Anandjiwala, R.D., *Simulation of airflow in nozzle-ring spinning using computational fluid dynamics: study on reduction in yarn hairiness and the role of air drag forces and angle of impact of air current*, In: Textile Research Journal, 2008, 78, 5, 412–420

[8] Rengasamy, R.S., Kothari, V.K., Patnaik, A., *Airflow simulation in nozzle for hairiness reduction of ring spun yarns. Part I: Influence of airflow direction, nozzle distance, and air pressure*, In: Journal of the Textile Institute, 2006, 97, 1, 89–96

[9] Han, C., Xue, W., Cheng, L., *Theoretical analysis on the yarn twist mechanism of self-twist jet vortex spinning*, In: Textile Research Journal, 2016, 86, 9, 911–918

[10] Kim, S E., Choudhury, D., *A near-wall treatment using wall functions sensitized to pressure gradient*, In: Separated and complex flows-1995, 1995, 85, 1, 273–280

[11] Han, C., Xue, W., Cheng, L., *Comparative analysis of different jet vortex spinning hollow spindle groove structures on yarn mechanism and yarn properties*, In: Textile Research Journal, 2016, 86, 19, 2022–2031

[12] Li, M., Yu, C., Shang, S., *Effect of vortex tube structure on yarn quality in vortex spinning machine*, In: Fibers and Polymers, 2014, 15, 8, 1786–1791

Authors:

JIANG YAN, HUA QIU

Jiangnan University, Faculty of Key Laboratory of Eco-Textiles, Ministry of Education, Wuxi-214122, Jiangsu-China

e-mail: 849267023@qq.com, qiuhua@jiangnan.edu.cn

Corresponding author:

HUA QIU

e-mail: qiuhua@jiangnan.edu.cn